

## ON THE DETECTION OF DISTRIBUTED ROUGHNESS ON BALL BEARINGS VIA STATOR CURRENT ENERGY: EXPERIMENTAL RESULTS

Giuseppe CURCURÙ<sup>1</sup>, Marco COCCONCELLI<sup>2</sup>, Fabio IMMOVILLI<sup>2</sup>, Riccardo RUBINI<sup>2</sup>

<sup>1</sup> DTMPIG, University of Palermo, Palermo, Italy, [g.curcuru@unipa.it](mailto:g.curcuru@unipa.it)

<sup>2</sup> DISMI, University of Modena and Reggio Emilia, Reggio Emilia, Italy,

[marco.cocconcelli@unimore.it](mailto:marco.cocconcelli@unimore.it), [fabio.immovilli@unimore.it](mailto:fabio.immovilli@unimore.it), [riccardo.rubini@unimore.it](mailto:riccardo.rubini@unimore.it)

### Summary

This paper deals with the detection of distributed roughness on ball-bearings mounted on electric motors. Most of the literature techniques focus on the early detection of localized faults on bearing (e.g. on the outer ring) in order to determine the bearing life and to plan the bearing replacing. Localized faults can be detected because they have characteristic signatures which is revealed in the frequency spectrum of the vibration signal acquired by an external sensor, e.g. accelerometer. Unfortunately other faults exist which do not have a characteristic signatures and then they could not be foreseen accurately: e.g. the distributed roughness. In this paper the motor stator current energy is proposed as a fault indicator to identify the presence of the distributed roughness on the bearing. Moreover an orthogonal experiment is set to analyse, through a General Linear Model (GLM), the dependencies of the current energy to the roughness level, and two environmental conditions: the motor velocity and the loads applied externally. ANOVA investigates the statistical significance of the considered factors.

Keywords: bearing diagnostics, distributed roughness, ANOVA, GLM, induction motor.

## 1. INTRODUCTION

Rotating bearings are very important component in many industrial machines. Their failure can reduce drastically the system reliability producing heavy economic losses. With the development of modern sensor-driven systems, the monitoring of such critical components became possible. This gives the possibility to follow the evolution of the wear processes in real time.

We know from literature that bearing failures can be revealed by machine vibrations [1]. Spectral analysis is the most used methodology. It makes possible the identification of localized faults ( inner race, outer race, balls, cage faults) by their characteristic faults frequencies [2].

Predictive models for the monitoring of localized faults have been produced [3]. More recently emphasis has been given to diagnostic via stator current [4, 5, 6, 7, 8]. The identification of localized faults by stator current analysis presents many practical and economical advantages (e.g. it is not necessary to use external sensors).

Another emerging research interest is the generalized (not-localized) roughness [4, 9].

This is mainly generated in the industrial environments, for example: contaminations, lack or loss of lubrication, corrosion due to water or acids, dust, humidity, etc.

It is particularly difficult to identify this kind of faults by standard/established vibration or stator current analysis, because, generally, there are no characteristic fault frequencies at all. This has been verified in many research publications [4, 5].

In [10] the mechanism of propagation of bearing vibrations to stator current signals via torque fluctuations has been investigated.

In [5, 11] new methodologies were proposed for the identification of generalized roughness faults, respectively employing mean spectrum deviation (MSD) and spectral kurtosis energy ( $E_{SK}$ ).

In this paper we present the main results of our study on simulated generalized roughness on the bearing rolling elements. In the present work we have hypothesized, using a General Linear Model, an interpretative model of the degradation stochastic process without considering the vibration of the machine, but only involving the stator current energy.

The paper is organized as follows. Chapter two introduces the experimental plan and the used machine. In chapter three we propose the data analysis and the interpretative model. The conclusions and the presentation of next research steps close the paper.

## 2. EXPERIMENTAL PLAN

The experimental plan is set to analyse dependencies of the stator current energy to the main parameter of interest, which is the roughness level of the spheres surface of the bearing, and two other environmental conditions: the angular velocity of the motor and the external radial load applied to the bearing.

A test-rig is available which is composed by: an induction machine on whose shaft is mounted the bearing under test, a mechanical system which externally loads the bearing and digital data

acquisition system that records the significant signals (vibration, current, etc.) characteristics.

The motor employed in the experiments is a 1.1 kW three phase induction machine with  $V_{rms}=380V$ ,  $N_b=28$  rotor bars,  $P=2$  poles pair. Rated slip and frequency are  $s_r=7\%$  and  $f_r=50Hz$ .

The ball-bearing under test is mounted on the shaft of the motor and it is externally loaded due to 8 identical springs working in parallel (Clamped between two parallel plates). The elastic coefficient of each spring is  $K_e=5.405$  N/mm. As a consequence of working in parallel, all springs are equivalent to a single spring with an equivalent elastic coefficient  $K_{e_{eq}}=43.24N/mm$ . The load is transferred to the ball-bearing through an apposite seat in order to distribute it along half part of the bearing. The given load is measured through the distance of separation of the two plates with respect to their unloaded configuration.

The bearing chosen for the test is a SKF 1205 ETN9 double crown self-aligning ball bearing with plastic cage. It was chosen in order to realize a quick and reliable disassembly to completely access each component. The bearing parameters, taken from the datasheet, are: outside diameter 52 mm, inside diameter 25 mm, 2 races on the inner ring with 13 balls for each race (26 balls total),  $D_c = 39.06$  mm,  $D_b = 7.45$  mm,  $\cos \beta = 1$ ,  $\beta = 0$  rad.

The ball contact angle  $\beta$  is estimated to be 0 because of the self-alignment characteristic of the bearing.

Each test of the experimental plan is performed on a batch of five bearing to increase the statistical meaning of the results. The different levels of each experimental factor are chosen according to Table 1, where the capital letter between parenthesis will be used to point each factor.

### 2.1. Roughness level (R#)

In order to simulate a distributed roughness on the bearing surface, each bearing is disassembled and the spheres cleaned from the lubricating oil. Only the spheres are then dipped into a concentrated solution of ferric chloride ( $FeCl_3$ ) salt for a given time. In particular four different roughness levels are considered:

- level R1: new spheres.
- level R2: one hour immersion in ferric chloride.
- level R3: two hours immersion in ferric chloride.
- level R4: three hours immersion in ferric chloride.

### 2.2. External load level (L#)

Four different radial load conditions are considered. The load is set by the compression of the eight springs between two plates and their displacement is measured with a Mitutoyo<sup>®</sup> digital caliper. The four load steps used in the tests, together with the corresponding displacements are:

- level L1: unloaded case. Springs not compressed.
- level L2: applied force of 411.84 N due to springs compression of 10mm.

- level L3: applied force of 844.64 N due to springs compression of 20mm.
- level L4: applied force of 1277.4 N due to springs compression of 30mm.

### 2.3. Motor angular velocity level (W#)

Three different velocities are chosen:

- level W1: 300 rpm (rotational frequency: 5 Hz)
- level W2: 900 rpm (rotational frequency: 15 Hz)
- level W3: 1500 rpm (rotational frequency: 25 Hz)

Table 1. Experimental factors levels summary

Level #	Experimental factor		
	Roughness [R#]	Load [L#]	Velocity [W#]
1	0 hours	0 N	5 Hz
2	1 hours	411.84 N	15 Hz
3	2 hours	844.64 N	25 Hz
4	3 hours	1277.4 N	

### 2.4. Acquisition system

An amperometer clamp placed on power cable of the motor is used to acquire the current data, which is sampled at 20 kHz by dSpace<sup>®</sup> 12 bit acquisition system for a period of 10 seconds. The current energy is calculated in Matlab<sup>®</sup> as the integration of the amplitude square value of the Fast Fourier Transform of the current signal as in Equation (1).

$$E_{cur} = \int_{-\infty}^{+\infty} |i(t)|^2 dt \quad (1)$$

The test is carried out as follow: all the bearing in the given test batch are opened and all their spheres are cleaned and degreased from the protective oil. Then the spheres of each bearing are etched using fresh solution, afterwards each bearing is reassembled and mounted on the motor shaft. The induction motor used during test was ran unloaded, e.g. was not connected to a brake or other type of load. For each radial load level the current signal is acquired at the different prescribed rotating speed. After these tests the bearing is disassembled and the next one is put under test and so on until the end of the experimental plan.

The total amount of tests is:

$$5 [\text{replications}] \times 4 [\text{roughness levels}] \times 4 [\text{load levels}] \times 3 [\text{velocity levels}] = 240 \text{ tests.}$$

Figures 1–3 show the current energy level calculated for each test is reported with respect to a specific characteristic. Figure 1 in particular shows the influence of load levels, Figure 2 and Figure 3 respectively present the roughness levels and the velocity levels.

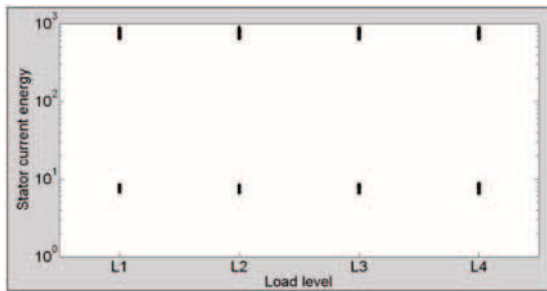


Fig. 1. Current energy [Joules] vs. load level

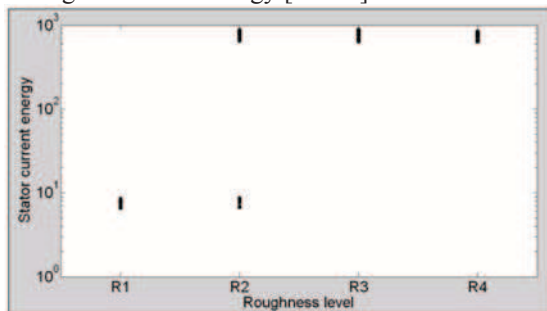


Fig. 2. Current energy [Joules] vs. roughness level

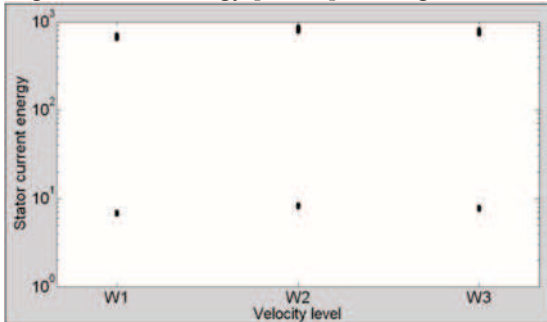


Fig. 3. Current energy [Joules] vs. velocity level

### 3. ANALYSIS OF THE EXPERIMENT

As outlined in the introduction, the presence of a distributed fault is characterized by the absence of characteristic fault frequencies both in the vibration and in the current spectra.

Nevertheless, looking at the current spectra obtained in the different simulated roughness levels, it is possible to appreciate a significant difference in the amplitude of the spectral lines.

The spectra reported – Figures 4-8 – below are referred to specific operational conditions and to the first two simulated roughness levels (R1, R2) in the frequency band [0,300]Hz.

Varying the operational conditions, both the shape of the spectra and their frequency content heavily change. In general it is possible to observe an increase in all components and even new spectral lines related to the different speeds. Nevertheless, in any operational condition, the spectra representing the four roughness levels (R1 – R4) are distinguishable. For this peculiarity we have chosen the absorbed stator current energy – during the 10 seconds of acquisition time – to characterize each roughness level in each operational condition.

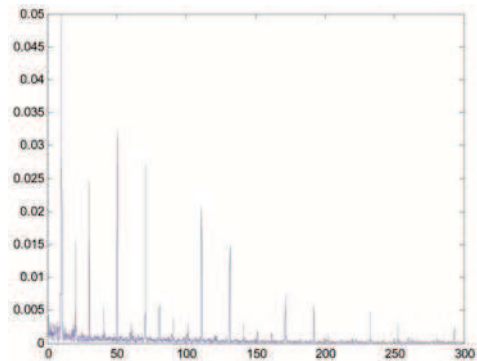


Fig. 4. Current spectrum for R1-L1-W1 test

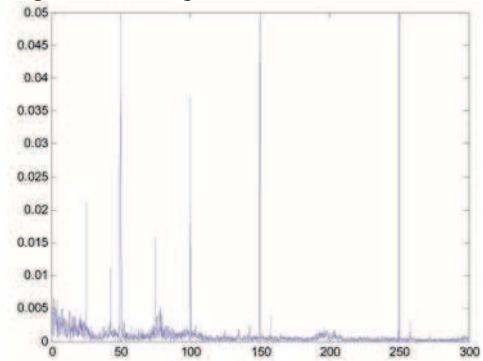


Fig. 5. Current spectrum for R1-L4-W3 test

In fact, changes in the current spectra (broadband changes, new spectral lines, increase of amplitudes, etc.) inevitably express a different energetic content. After calculating the energies at the different operational conditions, a statistical analysis of the data was produced.

We have considered the General Linear Model (GLM) to express energy  $Y$  as a linear combination of the three considered factors – roughness, speed, load – and, if possible, of the crossed factors.

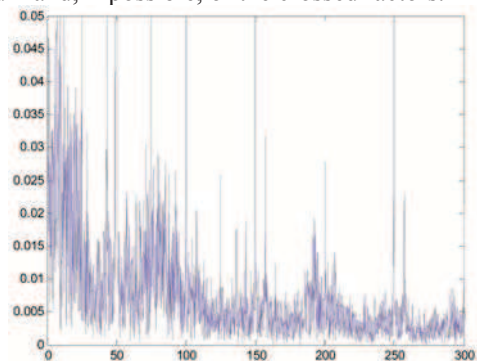


Fig. 6. Current spectrum for R2-L4-W3 test

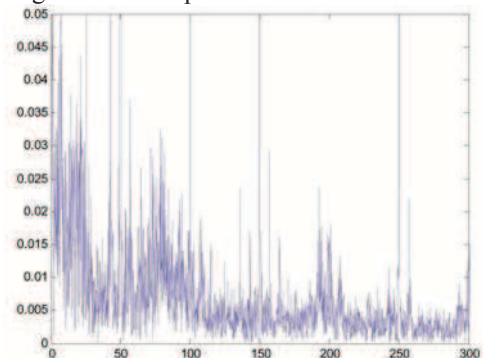


Fig. 7. Current spectrum for R3-L4-W3 test

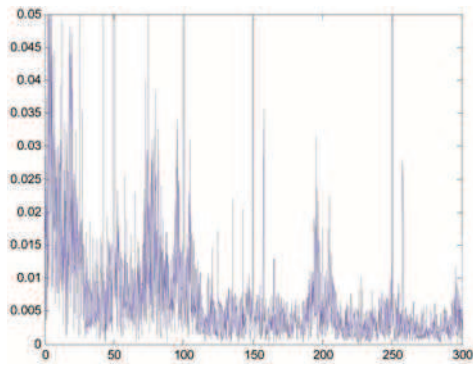


Fig. 8. Current spectrum for R4-L4-W3 test

A new experimental factor was added to the first three ones introduced before. This was the block factor *bearing* nested into the factor roughness. In fact, even if every bearing has the same nominal roughness level (the immersion time in the ferricchloride solution is the same for each bearing for each considered roughness level), it will inevitably exhibit a different effective roughness level. For this reason, trials cannot be considered as replications.

The following model was suggested:

$$Y_{ijklm} = \mu + \alpha_i + \beta_j + \gamma_k + \delta_{lk} + \alpha_i\beta_j + \alpha_i\gamma_k + \beta_i\gamma_k + \alpha_i\beta_j\gamma_k + \varepsilon_m \quad (2)$$

Where:

$\mu$  – is the general mean of the energies  $Y$ ;

$\alpha_i, \beta_j, \gamma_k$ , - are the principal effects of factors: speed, load and roughness.

The remaining two and three factors terms are representative of the interactions among the three factors;

$\delta_{lk}$  is the block factor bearing nested into factor roughness. Considered that the model is not deterministic, an error term  $\varepsilon_m$  was introduced. For this variable we made these assumptions: independence, normality and homogeneity of variance.

Using MINITAB<sup>®</sup>, the original data  $Y$ s have been analyzed. The analysis of residuals was made to verify the hypotheses of normality and homogeneity of variance.

The normal probability plot of the residuals is shown in Figure 9. For the original data, we obtained not normalized residuals because points are not sufficiently aligned along the blue line.

Not considering the outliers, the normal plot looks like a sigmoid. This shape is typical for those phenomena that exhibit a multiplicative behaviour and not an additive one.

This implies that the random variable must be lognormal.

Making a logarithmic transformation of the original data, GLM was applied to these transformed data. Therefore, the new variable is  $\log(Y)$  where  $Y$  is the stator current energy.

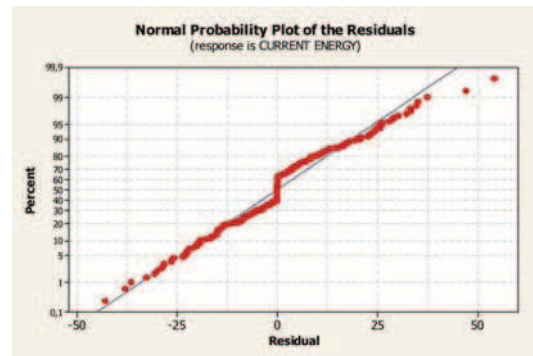


Fig. 9. Normal plot of the residuals for the original data (stator current energy)

The analysis of residuals for the transformed variable shows a rectification of the residuals' normal plot and evidences, at the same time, the presence of some outliers (beyond  $\pm 3\sigma$ ), as shown in Figure 10.

The analysis of variance (ANOVA) technique provides a statistical procedure to evaluate the contribution of the involved factors and their interactions to the variability in the response variable  $\log(Y)$ .

The ANOVA for the our data is reported in Table 2.

The ANOVA is used to test the significance of regression.

The F column of Table 2 shows both the results of the F-test on the factors and their interactions. The greater the F value, the more significant is the factor. This means that the *null hypothesis* is rejected. In this case the p-value is less than the threshold, that we set equal to 0,05.

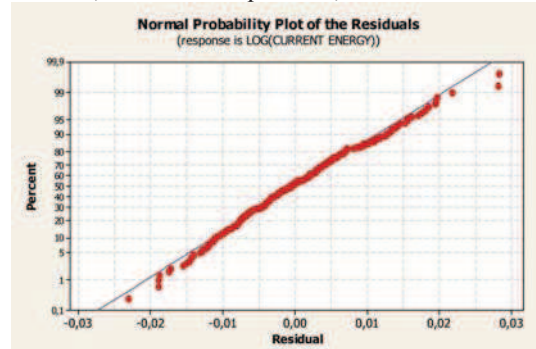


Fig. 10. Normal plot of the residuals for the data logarithmic value (stator current energy)

Table 2. ANOVA of the initial model

Source	DF	Seq SS	Adj SS	Adj MS	F	P
R	3	205,8647	189,9579	63,3193	715046,27	0,0000
L	3	0,0104	0,0023	0,0008	8,52	0,0000
W	2	0,3536	0,3389	0,1694	1913,34	0,0000
R*L	9	0,0025	0,0021	0,0002	2,67	0,0060
R*W	6	0,0009	0,0009	0,0002	1,70	0,1220
L*W	6	0,0010	0,0010	0,0002	1,86	0,0890
R*L*W	18	0,0007	0,0007	0,0000	0,43	0,9810
bearing(R)	16	0,0099	0,0099	0,0006	6,97	0,0000
Error	214	0,0190	0,0190	0,0001		
Total	277	206,2627				



Table 3. ANOVA of the simplified model

Source	DF	Seq SS	Adj SS	Adj MS	F	P
R	3	205,865	197,7228	65,908	745538,16	0,0000
L	3	0,0104	0,0023	0,0008	8,49	0,0000
W	2	0,3536	0,3532	0,1766	1997,69	0,0000
R*L	9	0,0025	0,0026	0,0003	3,21	0,0001
bearing(R)	16	0,0099	0,0099	0,0006	6,97	0,0000
Error	214	0,0216	0,0216	0,0001		
Total	277	206,263				

The interactions R\*W, L\*W, R\*L\*W in Table 2 are not statistically significant. Table 3 shows the ANOVA for the final model, where these interactions were eliminated.

ANOVA suggests the importance of speed, load and, most of all, of roughness. The only significant interaction is that between load and roughness.

The block factor *bearing* nested into the factor roughness must be considered as a technological factor and it can be omitted from a possible predictive model.

In conclusion the results of the experimental plan proves that interaction model in the equation (2) has to be changed and the new model is reported in equation (3).

$$Y_{ijkm} = \mu + \alpha_i + \beta_j + \gamma_k + \beta_i \gamma_k + \epsilon_m \quad (3)$$

#### 4. CONCLUSIONS

In this paper the use of the stator current energy as an indicator of the presence of distributed faults on ball-bearing has been investigated.

An experimental plan is set up to analyse the dependencies of the current energy both to bearing roughness level and to environmental conditions.

Two factors are considered as environmental conditions: the motor velocity and the radial load applied externally to the bearing.

The obtained interpretative model proves that it is possible to employ the stator current energy to monitor the degradation level of bearings once the operational conditions are known.

Future research activities are focused on:

- 1) identification of a quantitative/predictive model by building an adequate experimental design, in which stator current energy can be expressed as a linear combination of the experimental factors with numeric coefficients;
- 2) trying to extract from the stator current spectra new parameters mostly influenced by the roughness level and less dependent from the operational conditions.

#### 5. ACKNOWLEDGMENT

The authors acknowledge Prof. Alberto Lombardo (University of Palermo) for his help and invaluable suggestions.

#### 6. REFERENCES

- [1] Jayaswal P., Wadhvani A. K., Mulchandani K. B.: *Machine Fault Signature Analysis*, Int. J. Rot. Mach. (2008).
- [2] Kamarainen J. I., Lindh T., Ahola J., Kalviainen H., Partanen J.: *Diagnosis Tool for Motor Condition Monitoring*, IEEE Trans. Ind. Appl. 41 (2005) 963–971.
- [3] Harris T. A.: *Rolling Bearing Analysis*, John Wiley and Sons, New York, 2001.
- [4] Stack J., Habetler G., Harley G.: *Fault Classification and Fault Signature Production for Rolling Element Bearings in Electric Machines*, IEEE Trans. Ind. Appl. 40 (2004) 735–739.
- [5] Stack J., Habetler G., Harley G.: *Bearing Fault Detection via Autoregressive Stator Current Modelling*, IEEE Trans. Ind. Appl. 40 (2004) 740–747.
- [6] Zhou W., Habetler T., Harley R. G.: *Stator Current-Based Bearing Fault Detection Techniques: A General review*, Proceedings of IEEE International Symposium on Diagnostics for Electric Machines, Power Electronics and Drives SDEMPED 2007, IEEE, Cracow, Poland, 2007, pp. 7–10.
- [7] Blödt M., Raison B., Rostaing G., Granjon P.: *Models for Bearing Damage Detection in Induction Motors Using Stator Current Monitoring*, IEEE Trans. on Ind. Electr., 55(2008) 1813–1822.
- [8] Bellini A., Franceschini G., Tassoni C.: *Monitoring of induction Machines by maximum covariance method for frequency tracking*, IEEE Trans. Ind. Appl. 42 (2006) 69–78.
- [9] Elfeky A., Masoud M., Arabawy I.: *Fault Signature Production for Rolling Element Bearings in Induction Motor*, Proceedings of Compatibility in Power Electronics CPE '07, IEEE, Gdańsk, Poland, 2007, pp. 1–5.
- [10] Bellini A., Immovilli F., Rubini R. and Tassoni C.: *Diagnosis of bearing faults of induction machines by vibration or current signals: A critical comparison*, Proceedings of Annual Meeting of Industry Applications Society IAS '08, IEEE, Edmonton, Canada, 2008.
- [11] Bellini A., Cocconcelli M., Immovilli F. and Rubini R.: *Diagnosis of mechanical faults by Spectral Kurtosis Energy*, Proceedings of Annual Conference of Industrial Electronics Society IECON'08, IEEE, Orlando, USA, 2008.